Chapter 3

Seamless Transfer of Virtual Synchronous Generator Using Virtual Synchronizing Torque Controller

3.1 Introduction

Synchronization is mandatory in VSG like a conventional SG. The objective of the synchronization is to obtain a seamless transfer of VSG from standalone to grid-connected mode without using any extra dedicated synchronizing units or PI controllers. This chapter introduces a virtual synchronizing torque controller that offers precise and smooth synchronization of VSG with the distribution grid. VSG is simulated in MATLAB/Simulink, and the hardware prototype of the suggested system is implemented in the research lab for an experimental study to verify the feasibility of the proposed algorithm. The efficacy of the control strategy in different operating modes and power changes is presented through simulation and experimental results. Also, the proposed method is compared with three different existing synchronization methods. The major achievements of the proposed algorithm are,

- The elimination of PI regulators reduces the numerical burden of the proposed synchronizing controller due to its straightforward layout.

- The proposed controller completely eliminates auxiliary synchronizing controllers such as PLLs and FLLs.

- Another hallmark of the proposed synchronizing controller is that it does not demand extra controllers to identify the islanding situation.

- Also, there is no need to shift the control algorithm during the transition between operating modes. So, it eliminates the need for static breakers.

- The proposed synchronization method is faster and smoother than PLL-based VSG and the existing self-synchronizing methods.

A brief outline of the chapter is as follows:

- The schematic and operating principle of the considered VSG are presented in Section 3.2.

- The proposed virtual synchronizing torque controller is presented in 3.3.

- The small signal stability of the proposed synchronizing controller-based VSG is presented in 3.4.

- The simulation results of the proposed control technique using the MATLAB platform are discussed in Section 3.5.

- Experimental results of the VSG prototype are discussed in Section 3.6.

- The conclusion is made in Section 3.7.

3.2 Virtual Synchronous Generator

The schematic representation of the VSG structure is depicted in Figure 3.1, where v_o, i_o & L_f indicate the output voltage, output current, and filter inductance of the VSG, respectively. L_g and v_g represent the grid interfacing inductance and grid voltage, respectively. Filter resistance and capacitance are denoted by R_f and C_f, respectively.

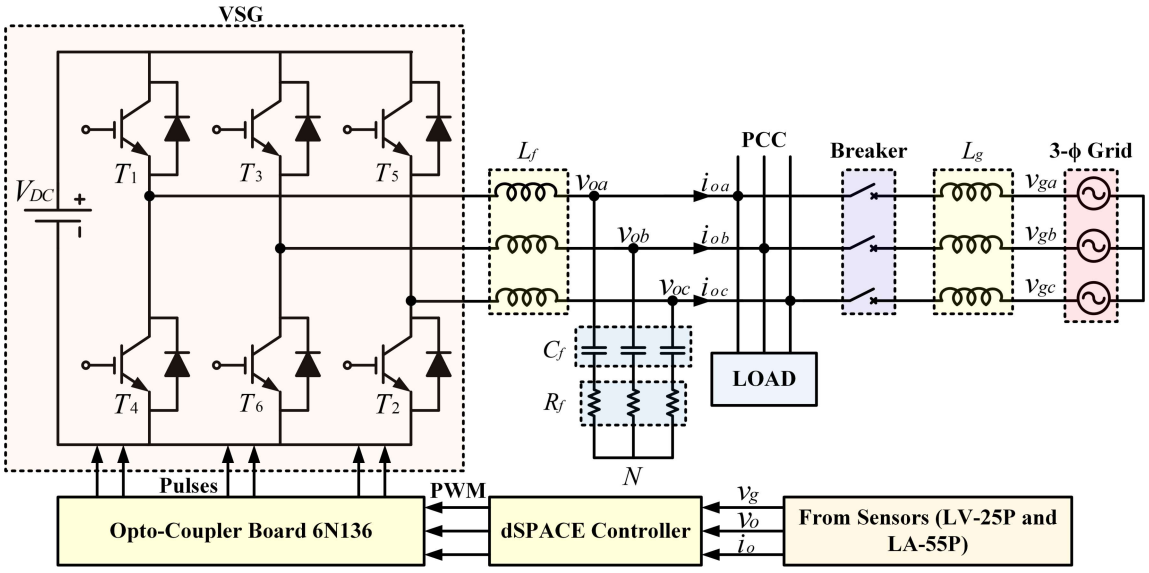

Figure 3.1: Virtual Synchronous Generator

The control algorithm for VSG comprises the properties of a synchronous generator, such as kinetic inertia and damping. Thus, equations (3.1) and (3.2) can be used to express the VSG equations.

$$T_m - T_e - D(\omega - \omega_0) = J\frac{d\omega}{dt} \tag{3.1}$$

$$\sqrt{2}E = k_{iq}\int (Q^* - Q) + \sqrt{2}D_q({V^*}_o - V_o) \tag{3.2}$$

Equation (3.1) reflects the VSG's active power loop, whereas equation (3.2) describes the reactive power loop. Here, D and J denote the virtual damping and the virtual inertia, respectively. The reference or mechanical torque of the VSG is T_m, and the torque generated by VSG is T_e. VSG rotor angle and angular velocity are denoted by θ and ω, respectively. ω_0 is the reference frequency. The number of poles is taken as 2. So, the mechanical speed and the electrical speed are the same. Reference active power is represented by P_m. VSG output active power P_e and frequency ω are used to determine the generated electrical torque T_e. Output voltage reference and actual output voltage are indicated by V_o^* and V_o, respectively, whereas E stands for the generated voltage reference. Output reactive power and the reference reactive power of VSG are Q and Q^*, respectively. The parameter k_{iq} is an integral gain, and D_q stands for the droop coefficient of the reactive power loop, which helps to regulate reactive power according to the voltage variation in the grid. T_D is the damping torque.

Complete VSG control algorithm with self-synchronization is shown in Figure 3.2. The primary components of VSG control remain unchanged.

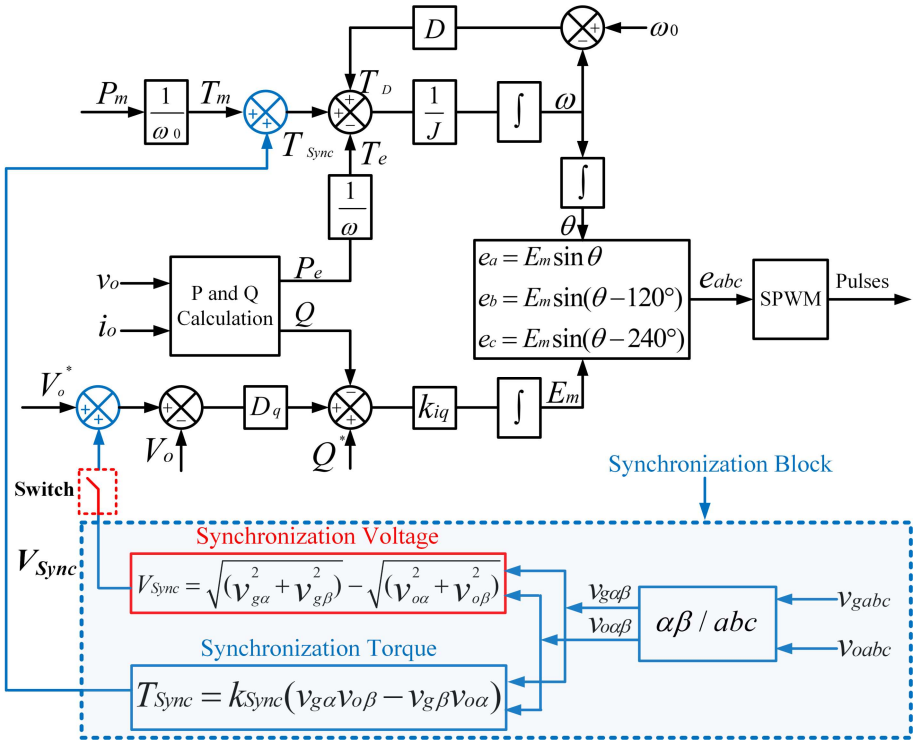

Figure 3.2: VSG with proposed synchronizing controller

3.3 Virtual Synchronizing Controller

VSG needs to be perfectly synchronized with the distribution grid to avoid any transients while synchrinizing. To do this, we must align the grid voltage with the VSG voltage's magnitude, angle, and frequency. For frequency and angle synchronization, a virtual synchronizing torque controller is suggested in the proposed control approach. A virtual synchronizing voltage controller is included to enhance the tracking performance of the VSG output voltage's magnitude to match the grid voltage. The proposed synchronizing controller is shown in Figure 3.3.

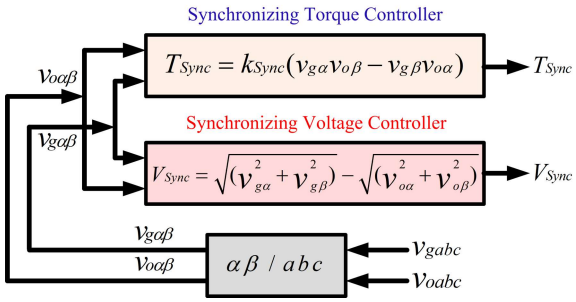

Figure 3.3: Proposed virtual synchronizing torque controller

3.3.1 Synchronizing Torque and Voltage Controller

Assume that the instantaneous phase voltages of the VSG and electrical grid are v_{oa} and v_{ga}, respectively. Let,

$$v_{ga} = V_g sin(\omega_g t + \theta_g) \tag{3.3}$$

$$v_{oa} = V_o sin(\omega_o t + \theta_o) \tag{3.4}$$

Here, V_o and V_g indicate the VSG output voltage and grid voltage amplitude, as shown in the Figure 3.4. For accurate synchronization, the phase difference $(\theta_g - \theta_o)$ and frequency difference $(\omega_g - \omega_o)$ must both be zero. The grid voltage and VSG output voltage's $\alpha\beta$ components are derived using Clarke's transformation, as shown below, to derive the suggested synchronizing controller.

$$\begin{aligned} v_{g\alpha} &= V_g sin(\omega_g t + \theta_g) \\ v_{g\beta} &= V_g cos(\omega_g t + \theta_g) \\ v_{o\alpha} &= V_o sin(\omega_o t + \theta_o) \\ v_{o\beta} &= V_o cos(\omega_o t + \theta_o) \end{aligned} \tag{3.5}$$

Figure 3.4 shows the $\alpha\beta$ components of both voltages.

Subtracting the multiplication of cross terms of supply voltage (v_g) and VSG voltage (v_o) yields the following,

$$v_{g\alpha}v_{o\beta} - v_{g\beta}v_{o\alpha} = V_o V_g sin[(\omega_g - \omega_o)t + (\theta_g - \theta_o)] \tag{3.6}$$

The mathematical expression $sin[(\omega_g - \omega_o)t + (\theta_g - \theta_o)]$ on the right side of the Eq.(3.6) has to be minimum to make the angle and frequency variation zero. A proportional gain

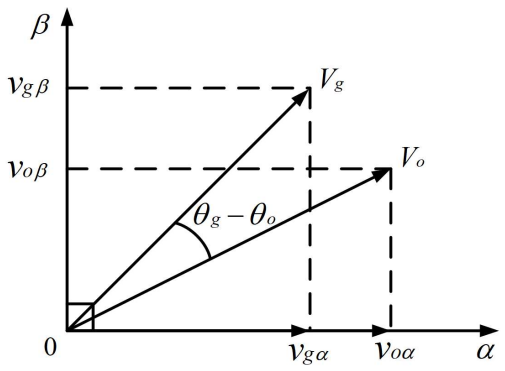

Figure 3.4: Grid and VSG voltage vector orientation

k_{Sync} is used to scale down equation (3.6) in order to determine the above-discussed virtual synchronizing torque. k_{Sync} is calculated by dividing the reference torque T_m by the square of the rated voltage because the synchronizing element is the torque here.

The idea behind the realization of the proposed controller is to adjust the reference mechanical torque T_m by adding the synchronizing component of torque T_{Sync} according to the change in frequency and phase of the grid. So, whenever there is a frequency or phase difference between grid and inverter output voltage, T_{Sync} is changed accordingly to make the error zero. As a result, the VSG frequency always remains the same as the grid frequency as long as the synchronizing torque is added to the reference torque T_m.

$$T_{Sync} = k_{Sync}(v_{g\alpha}v_{o\beta} - v_{g\beta}v_{o\alpha}) \tag{3.7}$$

To synchronize the frequency and angle of VSG with the grid, this virtual torque must be included in the reference torque T_m. Equation (3.8) is used to calculate the difference between the voltage magnitudes based on Figure 3.2.

$$V_g - V_o = \sqrt{(V_{g\alpha}^2 + V_{g\beta}^2)} - \sqrt{(V_{o\alpha}^2 + V_{o\beta}^2)} \tag{3.8}$$

The above relation yields the desired virtual synchronizing voltage that must be added to the output voltage reference in order to completely synchronize the VSG with the distribution grid. Hence, synchronizing voltage helps the VSG voltage amplitude track that of the grid in addition to phase and frequency. Therefore, equation (3.9) gives the virtual synchronizing voltage as

$$V_{Sync} = \sqrt{(V_{g\alpha}^2 + V_{g\beta}^2)} - \sqrt{(V_{o\alpha}^2 + V_{o\beta}^2)} \tag{3.9}$$

3.4 Small Signal Stability of the Proposed VSG

This section presents the small-signal model and dynamic stability study for the VSG incorporated with the proposed virtual synchronizing torque controller. Voltages, $\overline{V_g} = V_g\angle\theta_g$ and $\overline{V_o} = V_o\angle\theta_o$ are used to represent the phasors of the grid voltage and the capacitor voltage, respectively. δ is the power angle, which is expressed in the equation (3.10) as,

$$\delta = \int (\omega - \omega_g)dt = \theta_o - \theta_g \tag{3.10}$$

From Figure 3.4, the equations of the reactive and active power controller of VSG with a proposed synchronizing controller are expressed in equations (3.11)-(3.13) as

$$T_m - T_e + T_{Sync} - D(\omega - \omega_0) = J\frac{d\omega}{dt} \tag{3.11}$$

$$E_m = k_{iq}\int (Q^* - Q) + D_q({V^*}_o - V_o + V_{Sync}) \tag{3.12}$$

$$d\delta/dt = \omega - \omega_g \tag{3.13}$$

where, $T_{Sync} = 2k_{Sync}V_oV_gSin\delta$ and $V_{Sync} = V_g - V_o$.
Putting these values in Equation (3.11) and (3.12), we get:

$$T_m - T_e + 2k_{Sync}V_oV_gSin\delta - D(\omega - \omega_0) = J\frac{d\omega}{dt} \tag{3.14}$$

$$E_m = k_{iq}\int (Q^* - Q) + D_q({V^*}_o - 2V_o + V_g) \tag{3.15}$$

To examine small signal stability, the VSG small signal model can be derived around its steady-state operating points by linearizing equations (3.14) and (3.15). Any state variable x can be written as a summation of the corresponding steady-state operating point X_n and small ac variation $\tilde{x}$ as depicted in equations (3.16a)- (3.16f).

$$\omega = \omega_n + \tilde{\omega} \tag{3.16a}$$

$$\omega_0 = \omega_{0n} + \tilde{\omega_0} \tag{3.16b}$$

$$E_m = E_{mn} + \tilde{E_m} \tag{3.16c}$$

$$\delta = \delta_n + \tilde{\delta} \tag{3.16d}$$

$$V_o = V_{on} + \tilde{V_o} \tag{3.16e}$$

$$V_g = V_{gn} + \tilde{V_g} \tag{3.16f}$$

Since $\tilde{\delta}$ is very small, $\sin\tilde{\delta}$ is approximately equal to $\tilde{\delta}$, that is $\sin\tilde{\delta} \approx \tilde{\delta}$. And also, ω_0 is a constant value, hence $\widetilde{\omega}_0 = 0$. The variation in reference voltage is almost negligible. With properly designed voltage control, the capacitor voltage can accurately track the voltage reference. So, $V_o \approx E_m$. Neglecting all the DC quantities we have,

$$d\tilde{\omega}/dt = 1/J(\tilde{T_m} - \tilde{T_e} + 2k_{Sync}V_{on}V_{gn}\tilde{\delta} - D\tilde{\omega}) \tag{3.17}$$

$$d\tilde{E_m}/dt = k_{iq}\int(\tilde{Q^*} - \tilde{Q}) - 2D_q\tilde{E_m} \tag{3.18}$$

$$d\tilde{\delta}/dt = \tilde{\omega} \tag{3.19}$$

From equations (3.17)-(3.19), state space representation of the small signal model of VSG is written in matrix form as expressed in equation (3.20)

$$\dot{\tilde{x}} = A\tilde{x} \tag{3.20}$$

Where, $dx/dt = \dot{x}$ and $\tilde{x} = [\tilde{x_1} \quad \tilde{x_2} \quad \tilde{x_3}]^T$. Where, $\tilde{x_1} = \tilde{\omega}$, $\tilde{x_2} = \tilde{E_m}$ and $\tilde{x_3} = \tilde{\delta}$. State Matrix A is given in equation (3.21) as

$$A = \begin{bmatrix} -D/J & 0 & (2k_{Sync}V_{on}V_{gn})/J \\ 0 & -2D_qk_{iq} & 0 \\ 1 & 0 & 0 \end{bmatrix} \tag{3.21}$$

From the state matrix, A, dynamic performance and the stability of the proposed synchronizing controller for different parameters are analyzed using eigenvalue graphs. Eigenvalue plots from the state matrix A are depicted in Figure 3.5 (a)-3.5 (c).

Figure 3.5 (a) shows the eigenvalue plot of the VSG system for different values of D from 0.1 to 1.5. Eigenvalues (E_1, E_2, E_3) demonstrate the effect of the damping coefficient on the stability of the proposed controller. As shown in Figure 3.5(a), it is clear that increasing the value of D shifts all the eigenvalues of the system more toward the left side of the plane. Even for the small value of D, all eigenvalues have negative real parts. Hence, the system is stable for all the values of D. So, any value of $D > 0.1$ can be selected. Although choosing too big of a value of D will make the system more stable, more active power will be injected into the grid because of any frequency variation. So, there must be a trade-off when choosing D. So, D is selected as 1.1 here.

Eigenvalues of the system when inertia J is changed from 0.01 to 0.15 is shown in Figure 3.5 (b). Here, the system's eigenvalues give a clear insight into the influence of

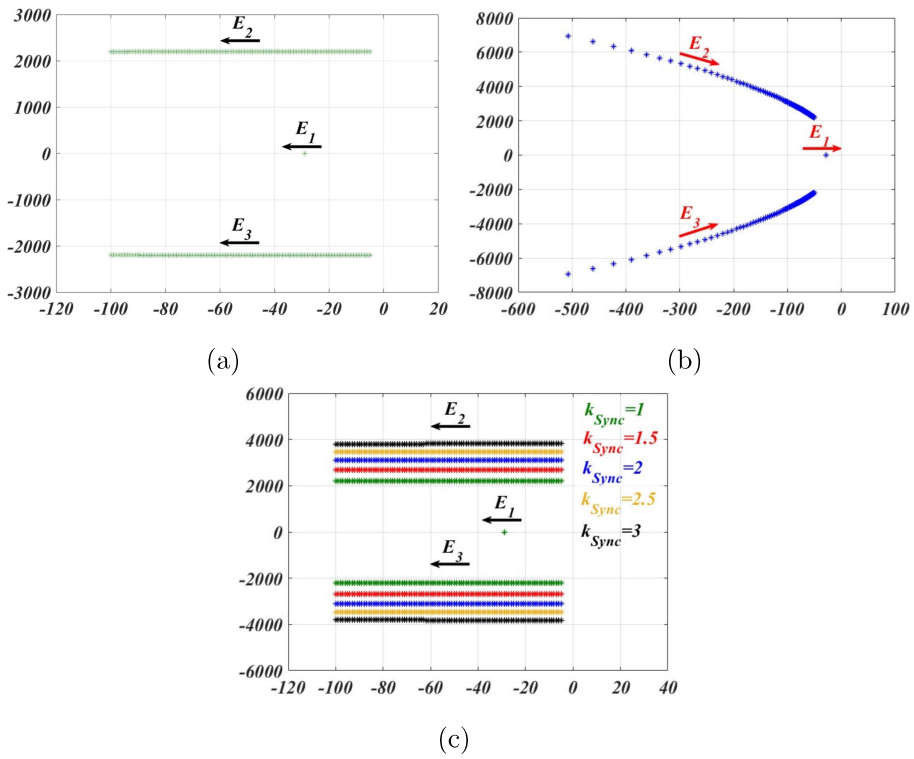

Figure 3.5: Eigen Value plots for (a) $D = 0.1 \rightarrow 1.5$ (b) $J = 0.01 \rightarrow 0.15$ (c) different values of k_{Sync} when $D = 0.1 \rightarrow 2$

J on controller performance. For large values of J, eigenvalues shift more towards the right side of the plane. It indicates that too much inertia can make the system less stable. Also, increasing J too much slows down the response of the power-frequency control loop due to the small bandwidth. Hence, large values of J should be avoided. Based on the eigenvalue plot, J is selected as 0.08.

The eigenvalue plot to analyze the effect of synchronizing gain k_{Sync} on the dynamic stability is shown in Figure 3.5 (c). For different values of k_{Sync}, D is changed from 0.1 to 2. It is observed that the eigenvalues of the system for any value of k_{Sync} lie on the left side of the plane when D is changed from 0.1 to 2. Increasing k_{Sync} only affects the imaginary part of the eigenvalue. Hence, big values of k_{Sync} result in increasing oscillations in system frequency during the synchronization process. Also, a higher value of D makes the system more stable, but more synchronizing power will be required. So, the proposed synchronizing torque controller-based VSG system is more stable for moderate synchronizing gain k_{Sync} and damping coefficient D. From Figure 3.5 (c), k_{Sync} is selected as 1.4.

3.5 SIMULATION RESULTS

VSG is simulated on the Matlab/Simulink platform. Grid voltage is considered 110 V/50 Hz. The simulated VSG system is shown in Figure 1. System parameters are given in Table 3.1. System behavior is observed during the synchronization process, after the grid connection, and for the seamless transfer between the grid connection and standalone mode. Following that, some of the currently used control methods are compared with the proposed control approach. Simulation results with detailed discussion are illustrated in the following subsections.

Table 3.1: System Parameters

S.No.	Parameter	Values
1	DC Voltage	220 V
2	3-ϕ ac Voltage	110 V
3	AC voltage frequency	50 Hz
4	Interfacing Inductance (L_f)	5 mH
5	Filter capacitance (C_f)	10 μF
6	Virtual Inertia (J)	0.08 $kg - m^2$
7	Virtual damping (D)	1.1 $N - m/rad/sec$
8	Synchronizing gain (k_{Sync})	1.4
9	k_{iq}	0.045
10	D_q	321 $Var/Volt$
11	Inverter switching frequency	10 kHz

3.5.1 Performance of the VSG system

Simulation results are used to validate the proposed synchronization controller. Results are shown in terms of the VSG output voltage (v_o), VSG current i_o, grid current i_g, VSG frequency f, VSG active power P_e, VSG reactive power Q, active and reactive power supplied by VSG to the grid P_g and Q_g, and synchronizing torque T_{Sync}.

The simulation began at $t = 0$. The circuit breaker was initially open. Initial settings for the grid voltage phase and frequency were 20 degrees and 49.9 Hz, respectively. As VSG is running in standalone mode, it supplies power only to the load.

3.5.1.1 Synchronization process

When the virtual synchronizing torque controller was turned on at $t = 0.5s$, VSG voltage was synchronized quickly with the grid voltage, as shown in Figure 3.6. The phase and frequency of the VSG output voltage follow the grid voltage parameters. Phase "A" of the grid and VSG voltage before and after synchronization is shown in Figure 3.6. Synchronizing torque is a virtual quantity calculated inside the control algorithm. Before

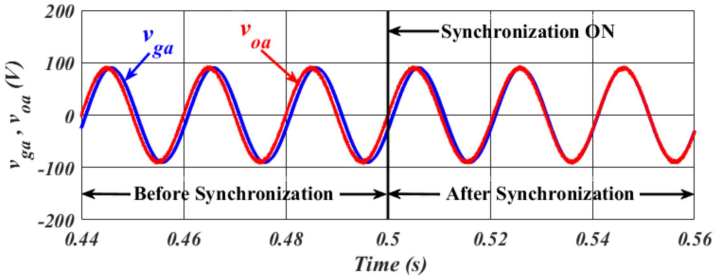

Figure 3.6: Grid and VSG voltage before synchronization and after synchronization

turning on the synchronizing controller, the VSG frequency was observed to be 50 Hz. But, once the synchronizing torque is applied, the VSG voltage frequency tries to match the grid frequency and settles to the same, i.e., 49.9 Hz. The frequency response of VSG with the synchronizing controller is shown in Figure 3.7. Synchronizing torque had a

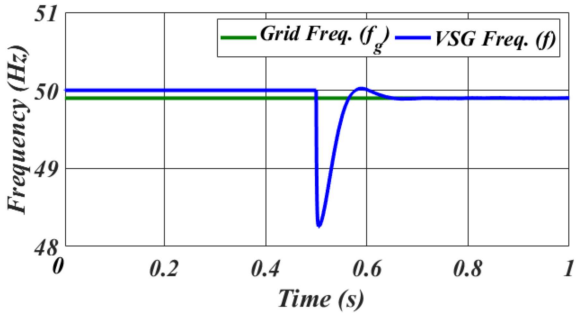

Figure 3.7: Synchronization of VSG and grid frequency

steady value of roughly 0.6 N-m prior to the interconnection of VSG and the grid. This synchronizing torque forces the phase as well as the frequency difference of the supply voltage and VSG voltage to zero. At this point, pre-synchronization of the VSG voltage and grid voltage is complete. Since the output voltage of the VSG is precisely synchronized with the grid, the synchronizing torque goes to zero as soon as the VSG integrates with

the grid. T_{Sync} is the compensating torque component to make the angle and frequency error to zero. In other words, it matches the power flow between VSG and the grid.

3.5.1.2 Grid connection

After the pre-synchronization process is done, the circuit breaker is closed at $t = 1.5s$, and VSG is interconnected with the grid. At this point, the operating mode of the VSG

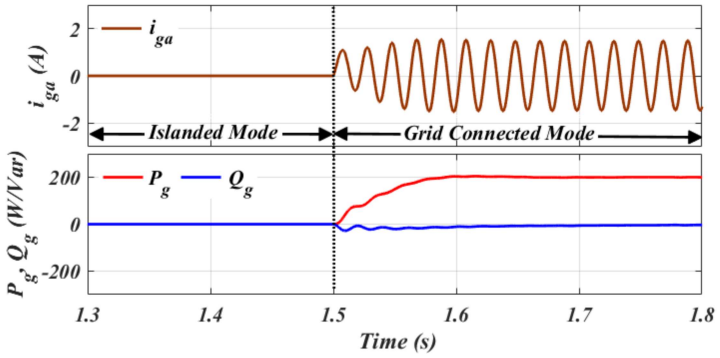

Figure 3.8: Current and power injected into the grid during mode transition

smoothly changes from standalone to grid-interfaced mode. It starts injecting approximately 200 W of compensating component of active power to the grid to nullify the phase and frequency difference between v_g and v_o to zero, as shown in Figure 3.8. Because of some amount of compensating power injection into the distribution grid, some grid current is observed at $t = 1.5s$. After the grid connection, the power flow between the grid and VSG is balanced. Hence, T_{Sync} reduces to zero gradually after closing the circuit breaker. So, there is no need to remove the synchronizing torque T_{Sync} because it is zero. Also, Figure 3.9 depicts the synchronizing torque before and after the grid integration.

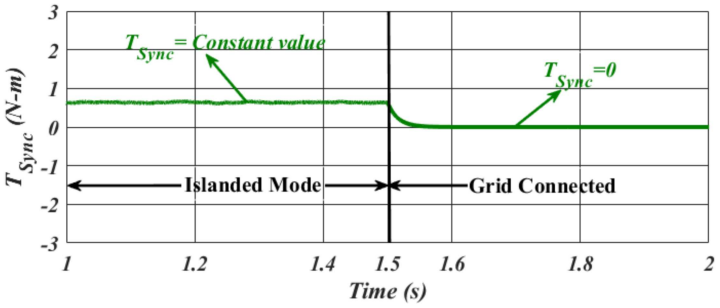

Figure 3.9: Behaviour of synchronization torque

3.5.1.3 Change in reference active power

Now, VSG is in grid-connected mode, so power flow between VSG and the utility grid can be maintained according to the reference power commands P_m & Q^*. At this point, 1 kW active power reference P_m was provided at $t = 2s$. Grid current starts increasing as the VSG starts to supply 1 kW of active power P_g to the grid, as shown in Figure 3.10. Reactive power Q_g during this time remains unchanged.

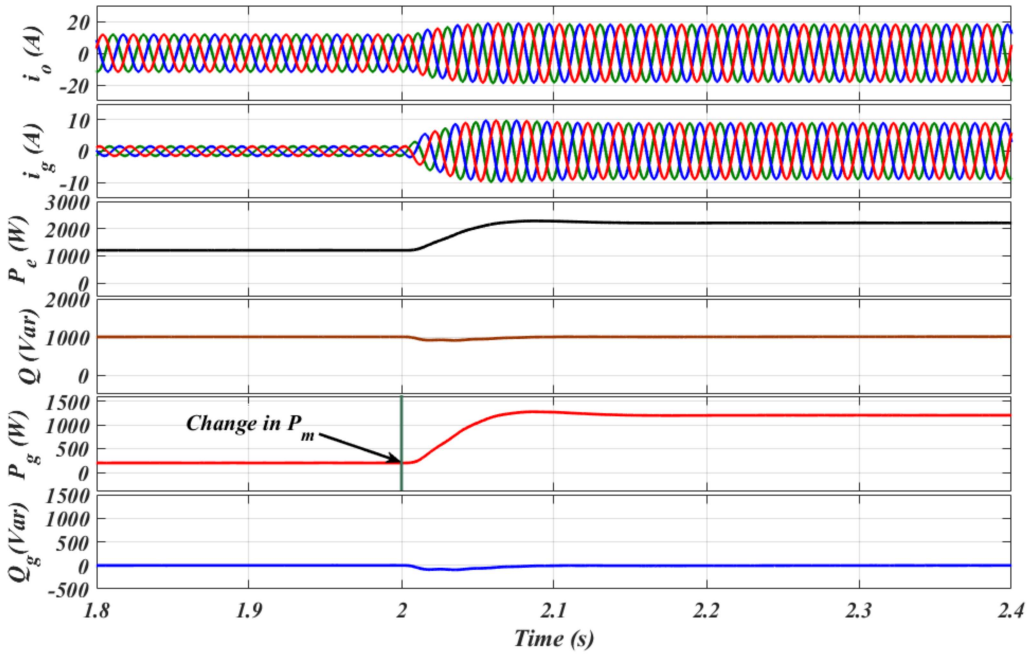

Figure 3.10: Active power injected by VSG into the grid with step change in reference active power P_m

3.5.1.4 Change in reference reactive power

Now, 1 kVar Q^* command was provided at $t = 2.5s$. Without disturbing the active power P_g, VSG starts injecting the reactive power Q_g into the grid, as shown in Figure 3.11.

3.5.1.5 Change in grid frequency

At $t = 3.5s$, the supply frequency was raised by 0.2 Hz, i.e., 50.1 Hz. Due to the frequency difference between VSG and grid voltage, i.e., $\omega_g - \omega_o$, damping torque component $T_D = D(\omega_g - \omega_o)$ comes into effect, and VSG exchanges a finite amount of active power with the grid as shown in Figure 3.12.

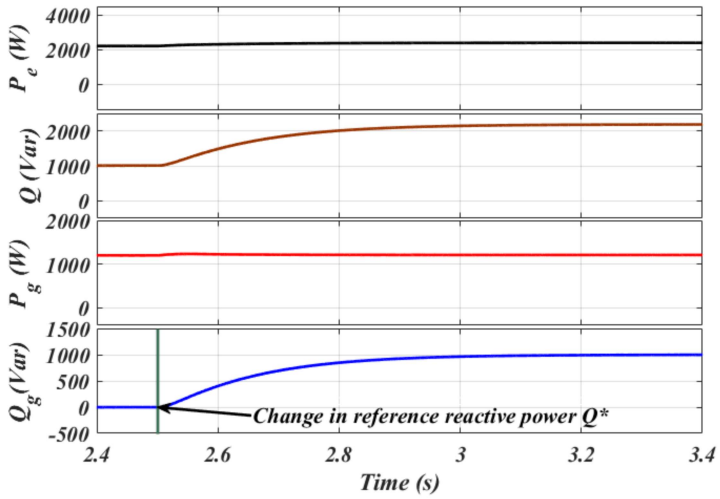

Figure 3.11: Reactive power injected by VSG into the grid with step change in reference reactive power Q^*

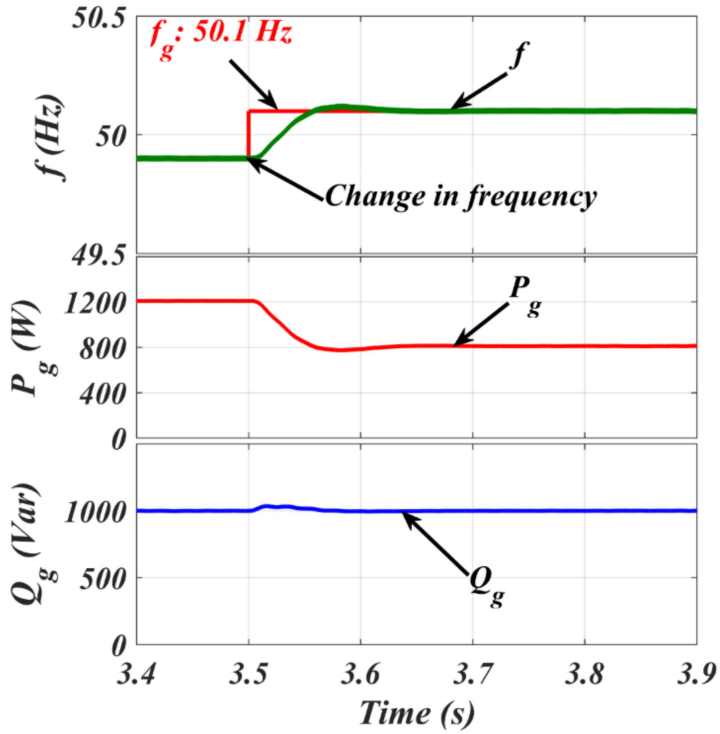

Figure 3.12: Active and reactive power flow between VSG and grid with change in grid frequency f_g

3.5.1.6 Grid disconnection

The grid was disconnected at $t = 4s$. A smooth transition of VSG from grid-connected mode to islanding mode occurred. Still, the VSG feeds to the load (i_o) even if the grid

current (i_g) becomes zero, as shown in Figure 3.13. The simulation was stopped at $t = 4.5s$.

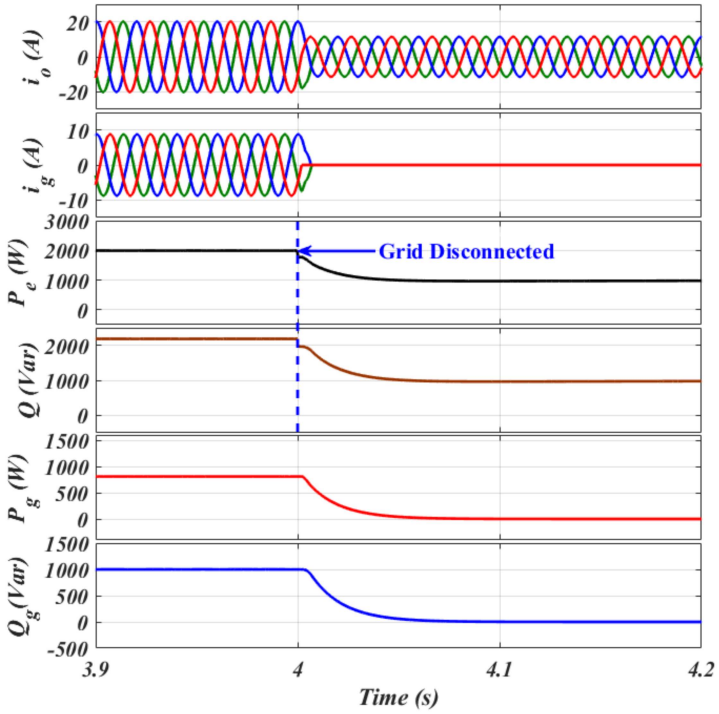

Figure 3.13: Grid current, VSG current, VSG active and reactive power, active and reactive power injected into the grid during grid-connected to islanded mode transition

The performance of the VSG with the proposed self-synchronizing method is shown in Figure 3.14.

With the suggested synchronizing torque controller, VSG operates in a proper manner to fulfill all the supplementary demands in the grid-tied mode. Switching of VSG from autonomous mode to the grid-interfaced mode is very smooth. We can identify the operating mode of VSG by just observing the value of T_{Sync}, which is useful in unintentional islanding situations. If T_{Sync} has some constant value, then VSG is in islanding mode. If it is zero, that means VSG is working in grid-tied mode. So, there is no need for separate control to check the islanding situations. And, since there is no need to turn off the synchronizing torque, we don't have to shift the control algorithm every time. Hence, there is no need for static circuit breakers, which makes the system more complex. Also, there is no overcurrent during the grid connection and islanding because the synchronizing torque controller will take care of it.

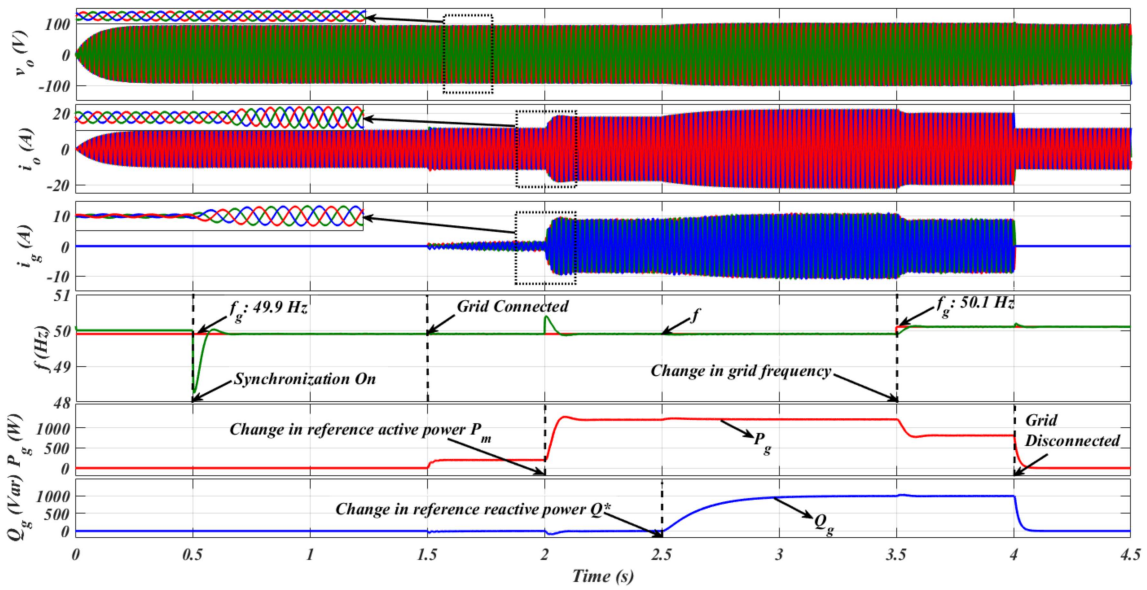

Figure 3.14: VSG Response with the proposed synchronizing controller

3.5.2 Comparison with currently used synchronization techniques

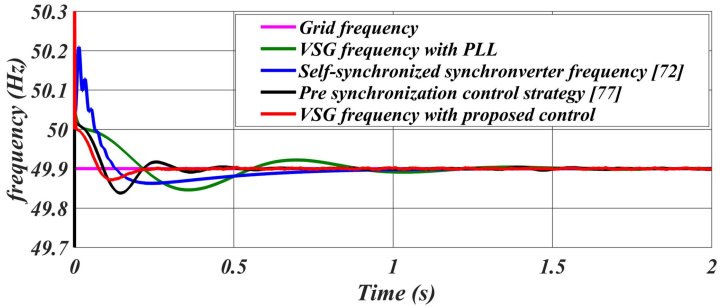

Figure 3.15: Frequency curves of VSG with various synchronization methods

This section compares the proposed controller's frequency tracking performance to that of a PLL, a self-synchronized synchronverter [72], and pre-synchronization control [77]. In Figure 3.15, the simulation results of frequency curves for all four methods are depicted in a comparative manner. In contrast to VSG with PLL, synchronverter [72], and pre-synchronization control [77], it is evident from Figure 3.15, that VSG with the suggested synchronizing controller reaches the grid frequency more quickly. Additionally, the proposed synchronization method has less frequency overshoot than the other three methods. Also, unlike the self-synchronized VSG [72], the proposed controller does not require solid-state switches to acquire the mode transition. The proposed controller does not need any PI controllers, unlike VSG with PLL. Hence, the controller has a less complex

structure. Table 3.2 provides a comparative analysis of the proposed method with the other three methods.

Table 3.2: Comparative Analysis

Features	VSG with PLL	Synchronverter [72]	Pre-Synchronization [77]	Proposed Method
PI Controllers	Yes	Yes	No	No
PLL	Required	No PLL	No PLL	No PLL
Islanding Detection Method	Required	Required	Not reported	Not required
Control Modifiations	Yes	Yes	No	No
Synchronization speed	Slow	Medium	Medium	Fast
Numerical Calculations	More	More	More	Less

3.6 EXPERIMENTAL RESULTS

The developed prototype is explained in Chapter 2. A power system analyzer (Fluke-1736 Power Logger) is used to record the steady-state output of the VSG system. The transient behavior of the VSG is recorded using a digital oscilloscope (KEYSIGHT in indivision DSOX2004A). The experimental results of the proposed VSG are presented in this section to show its superiority for both steady-state and dynamic conditions. Now, the proposed control algorithm is verified and the results are recorded.

3.6.1 Performance of VSG During Islanded Mode

Figure 3.16 shows the performance of VSG in islanded mode with linear loads. Figure 3.16(a)-(b) depicts the three-phase line voltages ($v_{oab}, v_{obc}, v_{oca}$) and output currents ($i_{oa}, i_{ob}, i_{oc}$) of VSG. Figure 3.16 (c) shows the harmonic spectrum of the VSG currents (i_{oa}, i_{ob}, i_{oc}). The THDs of the VSG currents are observed as 2.3%, 2.2%, and 2.2%, respectively. Figure 3.16 (d) shows the harmonic spectrum of the VSG voltages ($v_{oab}, v_{obc}, v_{oca}$). The THDs of the VSG voltages are observed as 2.4%, 2.2%, and 2.3%, respectively.

3.6.2 Synchronization Process

For the grid connection of VSG, synchronization control is activated to match the output voltage of VSG with the supply voltage. Figure 3.17 (a) shows the VSG voltage v_{oa} and grid voltage v_{ga} when pre-synchronization occurs prior to the shifting from off-grid mode

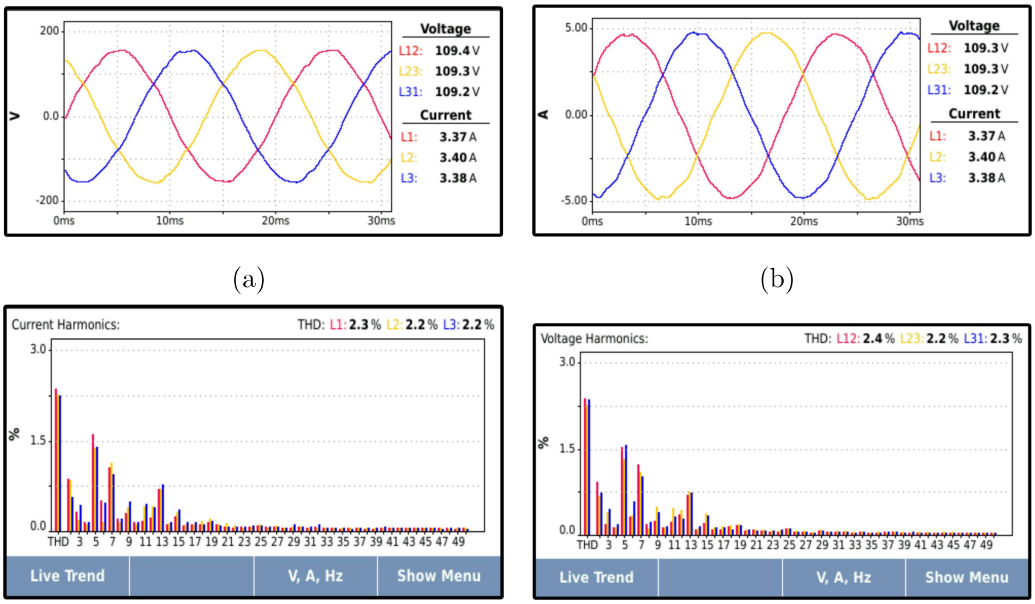

(a) (b)

(c) (d)

Figure 3.16: (a) Output voltage and (b) current waveforms of VSG, (c) Harmonic spectrum of VSG currents (i_{oa}, i_{ob}, i_{oc}) and (d) Harmonic spectrum of VSG voltages ($v_{oab}, v_{obc}, v_{oca}$) for an islanded mode.

to grid-on mode. The synchronization is shown with regard to the VSG line voltage (v_{oab}),

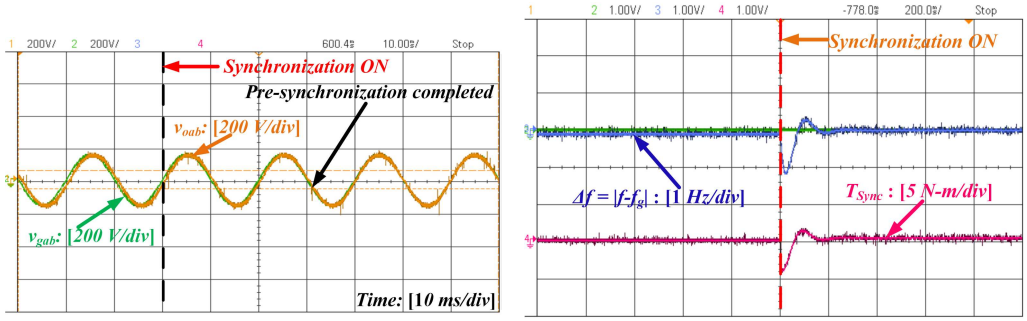

(a) (b)

Figure 3.17: (a) Synchronization of v_g and v_o and (b) Frequency error Δf and T_{Sync}

grid voltage (v_{gab}), frequency error ($\Delta f = f - f_g$), and synchronization torque (T_{Sync}). During islanded mode, VSG and grid voltage are not synchronized with each other, i.e., there is some phase difference between v_{gab} and v_{oab} as seen in Figure 3.17 (a). Also, a frequency error Δf of around 0.1 Hz exists between grid voltage and VSG voltage, as seen in Figure 3.17 (b). When the virtual synchronization torque controller is turned on,

the phase angle error between voltage v_{gab} and v_{oab}, i.e. $(\theta_g - \theta_o)$ becomes zero and both the voltages are perfectly synchronized with each other. The behavior of frequency error Δf and synchronizing torque T_{Sync} is shown in Figure 3.17 (b). The frequency difference between grid and VSG, i.e., Δf, becomes zero after some time. The synchronization torque T_{Sync} reaches some constant value after small oscillations, as depicted in Figure 3.17 (b). Once the angle and frequency of the distribution grid and VSG are synchronized with one another, the synchronizing gain decreases and eventually goes to zero.

3.6.3 Smooth Transition from Islanded Mode to Grid-Connected Mode

Post synchronization, VSG is interconnected with the grid. A smooth transition is observed. The transition of VSG from islanded mode to grid-connected mode is shown in Figure 3.18. As soon as the grid-interfacing circuit breaker is turned on, the synchroniz-

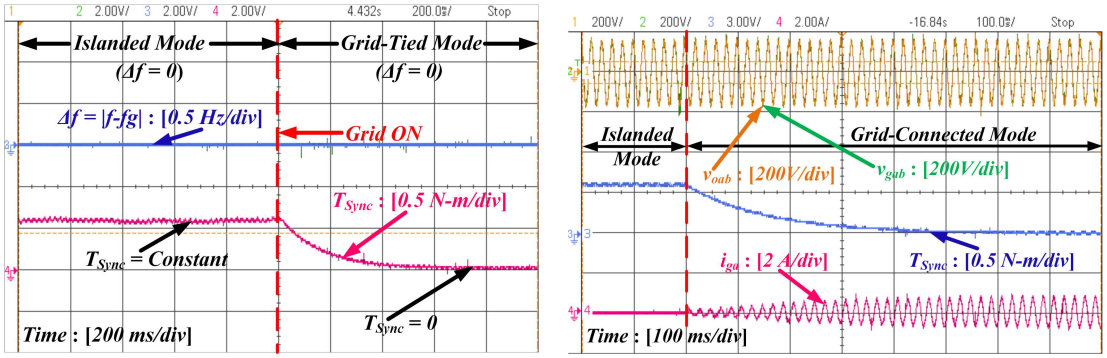

(a) (b)

Figure 3.18: VSG transition from islanding to grid connection (a) Δf, Synchronizing torque T_{Sync} and (b) v_{gab} and v_{oab} and i_{ga}

ing torque becomes perfectly zero after some time. There is no change in the frequency and phase of the VSG at this time because of the perfect synchronization, as seen in Figure 3.18 (a). Voltages v_{gab}, v_{oab}, T_{Sync} and i_{ga} are shown in Figure 3.18 (b). The VSG voltage is the same before and after the grid connection. Before grid connection, grid current i_{ga} can be seen as zero. After connection, a small grid current flows because of the synchronizing torque to make phase and frequency errors zero.

VSG voltage (v_{oab}), distribution grid voltage (v_{gab}), load current (i_{La}), and grid

current (i_{ga}) waveforms are shown in Figure 3.19. It is apparent that load current is maintained constant during the switching operation from standalone to grid-connected mode. Load is not affected during the transition of the operating mode. Once the

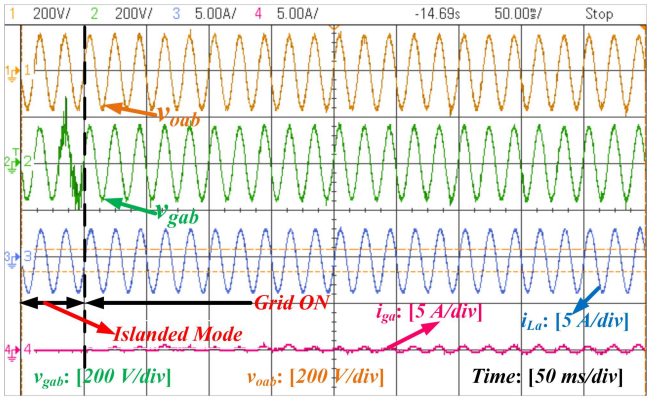

Figure 3.19: Waveforms of (a) v_{oab}; (b) v_{gab} (c) i_{La} and (d) i_{ga} during transition from islanded to grid-connected mode

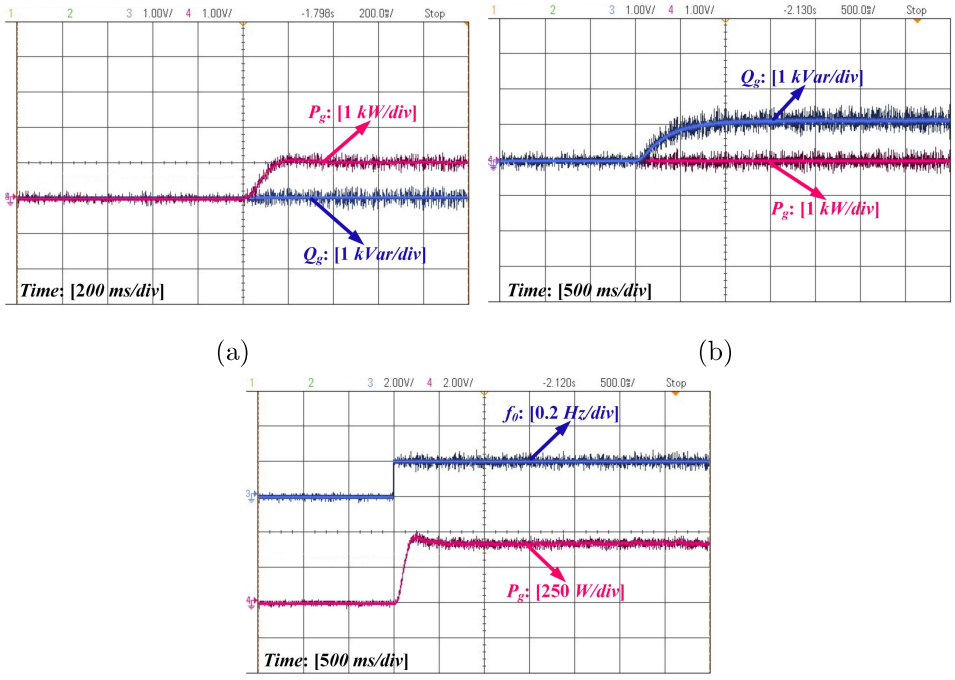

Figure 3.20: (a) Change in active power P_g with the reference active power P_m (b) Change in reactive power Q_g with the reference reactive power Q^* (c) Change in active power P_g with VSG reference frequency f_0

VSG starts operating in grid mode, its dynamic performance is observed by changing

the reference active and reactive power commands and the VSG frequency. Initially, the active power reference P_m to the grid is increased from 0 to 1 kW, as depicted in Figure 3.20 (a). The active power exchange between VSG and the grid starts occurring, and there is no change in reactive power. Now, reactive power reference Q^* to the grid is changed from 0 to 1 kVar, assuming that there is no variation in active power reference and frequency. VSG quickly supplies the reactive power Q_g to track the reactive power command, as shown in Figure 3.20 (b).

The behavior of the VSG is observed for frequency regulation by changing the VSG reference frequency (f_0). VSG performs the frequency regulation by supplying or absorbing the active power to the grid. The variation of active power generated from VSG when the reference frequency is increased by 0.2 Hz is shown in Figure 3.20 (c).

3.6.4 Transition from Grid Connected to Islanded Mode

Grid voltage v_{gab}, VSG voltage v_{oab}, load current i_{La} and grid current i_{ga} during the transition from grid-connected to islanded mode are shown in Figure 3.21. There is a

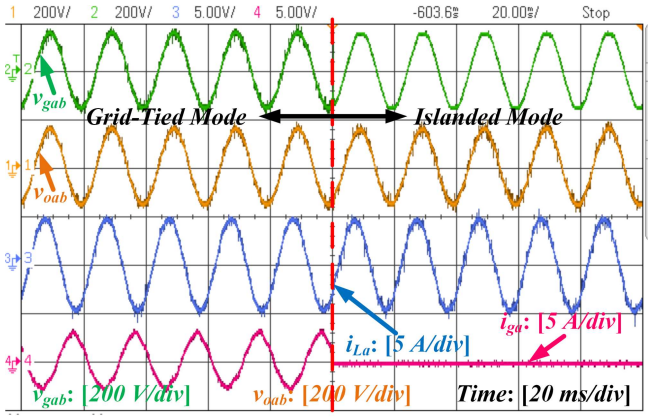

Figure 3.21: v_{gab}, v_{oab}, i_{La} and i_{ga} during grid to islanded mode transition

smooth transition in the magnitude of VSG output voltage and load current. During grid-connected mode, some finite amount of grid current i_{ga} was flowing. As soon as the grid is disconnected from VSG, the grid current becomes zero, but load current i_L is still maintained. Hence, there is a seamless transfer of VSG between grid-connected and islanded modes.

3.6.5 Performance with the non-linear load

The proposed VSG system's performance is tested with a non-linear load. As a non-linear load, a diode bridge rectifier is connected at the PCC. Figure 3.22 shows the behavior of VSG voltage (v_{oa}), VSG current (i_{oa}), grid current (i_{ga}), and load current (i_{La}) for the non-linear load. The grid current is still maintained sinusoidal, even after the connection of the non-linear load. Hence, VSG supplies the current harmonic requirements of the load without affecting the grid power quality.

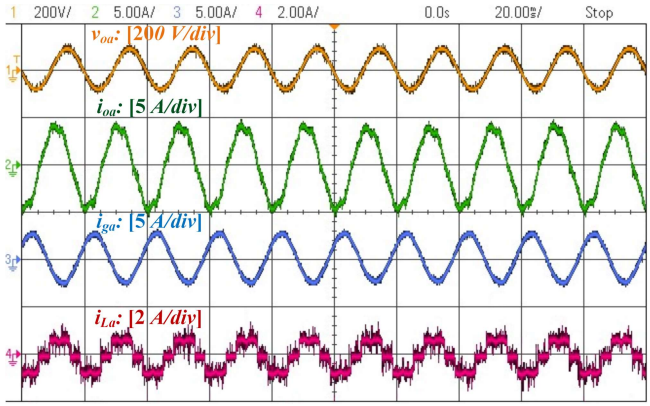

Figure 3.22: Behavior of v_{oa}, i_{oa}, i_{ga} and i_{La} with non-linear load

3.6.6 Comparison with already existing techniques

Figure 3.23 presents a comparison of the proposed method with the currently existing techniques. The frequency error between grid and VSG voltage with the proposed synchronizing controller during the synchronizing process is compared to the PLL-based VSG, synchronverter [72], and pre-synchronization control [77]. PLL-based VSG frequency oscillates more during the synchronization process and takes the longest time to make frequency error (Δf) to zero, as shown in Figure 3.23 (a). Self-synchronized synchronverter [72] also oscillates for some time but has less overshoot in frequency than PLL-based VSG, which is shown in Figure 3.23 (b). Pre-synchronization control [77] performs better than the PLL and synchronverter [72], as shown in Figure 3.23 (c). Still, VSG with the proposed virtual synchronizing torque-based controller is very fast in synchronization as compared to the other three methods and has the least frequency oscillations during synchronization, as shown in Figure 3.23 (d). Also, it does not require any separate algo-

rithms to identify the islanding situation. The value of synchronizing torque defines the mode of operation.

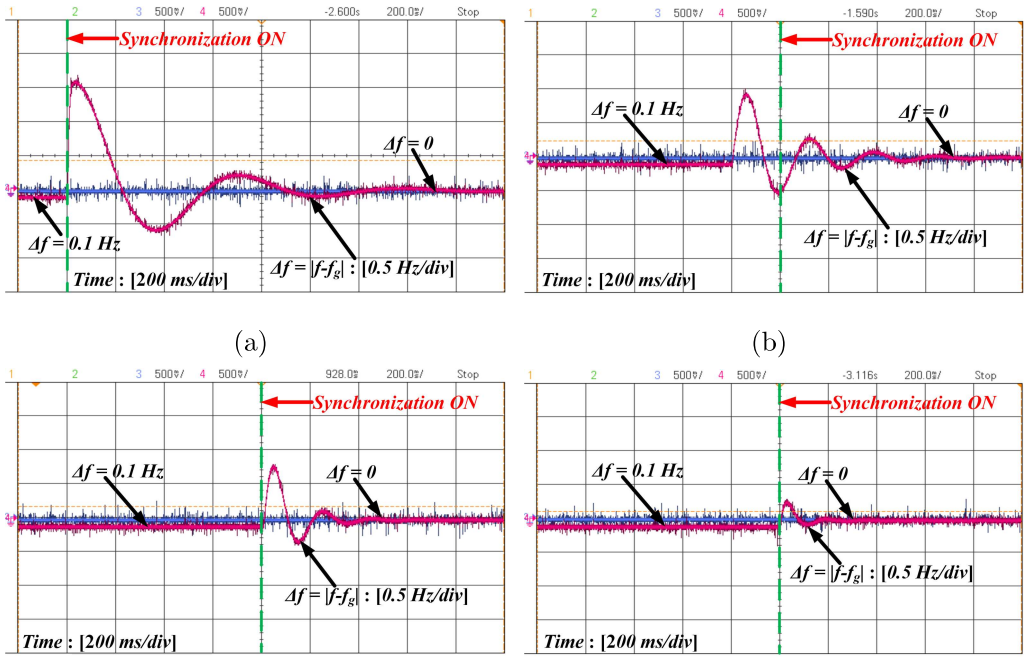

Figure 3.23: Frequency response of VSG with (a) PLL, (b) Self-synchronizing synchronverter [72], (c) Pre-synchronization [77], and (d) Proposed controller

3.7 Conclusion

For an effortless shifting of the VSG between the islanded and grid-tied modes, the voltage magnitude, frequency, and angle of the VSG must be identical to the supply voltage magnitude, frequency, and phase to suppress the huge amount of inrush current at the moment of breaker opening or closing. This chapter presents a virtual torque and voltage synchronization algorithm for the smooth integration of VSG with the utility grid. The controller has provided the necessary synchronizing torque to keep the frequency and angle mismatch between the utility voltage and the VSG voltage to a minimum. As a result, the frequency disturbances of the VSG during circuit breaker switching have been decreased. By tracking the grid voltage magnitude, virtual synchronizing voltage has reduced voltage amplitude error. Therefore, without employing any phase-locked loops, the

proposed control technique enhanced the performance of the VSG synchronizing action. Furthermore, the proposed controller eliminates the PI regulators from the outer loop, i.e., the power controller of VSG, which requires accurate parameter tuning, much like the complex and time-consuming process of PLL gains. Also, control modifications are not required during standalone or grid-connected modes. The proposed method requires no additional controller to identify the unwanted islanding situations because, the operating mode can be deduced from the synchronizing torque value. Also, the proposed synchronizing controller is compared with the three different synchronization methods, i.e., PLL-based VSG, synchronverter [72], and pre-synchronization control [77], and observed that the proposed synchronization method is faster than the other three methods and shows less overshoot in VSG frequency.